Research Square

Preprints are preliminary reports that have not undergone peer review.
They should not be considered conclusive, used to inform clinical practice,
or referenced by the media as validated information.

Temporal organization of the Plasmodium falciparum transcriptome prioritises genetic polymorphisms associated with artemisinin response

Andrew Walakira

adwalakira@gmail.com

The African Centre of Excellence in Bioinformatics and Data Intensive Sciences, Kampala, Uganda.

Andrew Walakira

The African Centre of Excellence in Bioinformatics and Data Intensive Sciences, Kampala, Uganda.

Ronald Galiwango

African Center of Excellence in Bioinformatics and Data-Intensive Science, Makerere University, Kampala, Uganda. Infectious Diseases Institute, Makerere University, Kampala Uganda

Brenda Namugamba

The African Centre of Excellence in Bioinformatics and Data Intensive Sciences, Kampala, Uganda.

Shahiid Kiyaga

Infectious Diseases Research Collaboration, Kampala, Uganda; Department of Immunology and Molecular Biology, College of Health Sciences, Makerere University, Kampala https://orcid.org/0000-0002-6380-4714

Kevin Cissy Nabukeera

The African Center of Excellence in Bioinformatics and Data-Intensive Sciences, Kampala, Uganda https://orcid.org/0009-0009-8319-1853

Syrus Semawule

The African Center of Excellence in Bioinformatics and Data Intensive Sciences, Kampala - Uganda https://orcid.org/0009-0004-3405-8099

Edith Nabukenya

The African Centre of Excellence in Bioinformatics and Data Intensive Sciences, Kampala, Uganda.

Joseph Nyanzi

The African Centre of Excellence in Bioinformatics and Data Intensive Sciences, Kampala, Uganda.

Martin Okitwi

Makerere University https://orcid.org/0000-0003-2712-2174

Stephen Orena

Infectious Diseases Research Collaboratio

Thomas Katairo

Infectious Diseases Research Collaboratio

Victor Asua
Institute for Tropical Medicine, University of Tübingen https://orcid.org/0000-0002-0489-4692

Stephen Tukwasibwe
Infectious Diseases Research Collaboration, Kampala

Grace Kebirungi
The African Centre of Excellence in Bioinformatics and Data Intensive Sciences, Kampala, Uganda.

Fredrick Kakembo
Makerere University

David Twesigomwe
Medical Research Council/Uganda Virus Research Institute and London School of Hygiene and Tropical Medicine Uganda Research Unit

Joaniter Nankabirwa
Makerere University

Emmanuel Arinaitwe
Infectious Diseases Research Collaboration

Karamoko Niaré
Brown University

Jessica Briggs
University of California, San Francisco https://orcid.org/0000-0002-8078-3898

Melisa D. Conrad
Johns Hopkins Malaria Research Institute

Isaac Ssewanyana
https://orcid.org/0000-0001-8605-2001

Moses Kamya
Makerere University https://orcid.org/0000-0001-9106-4234

Philip Rosenthal
UCSF https://orcid.org/0000-0002-7953-7622

Samuel Nsobya
Infectious Diseases Research Collaboration

Daudi Jjingo
The African Center of Excellence in Bioinformatics and Data-Intensive Sciences, Kampala, Uganda
https://orcid.org/0000-0003-1685-9234

Article

Keywords:

Posted Date: November 4th, 2026

DOI: https://doi.org/10.21203/rs.3.rs-11552900/v1

License: This work is licensed under a Creative Commons Attribution 4.0 International License.
Read Full License

Additional Declarations: There is **NO** Competing Interest.

Temporal organization of the *Plasmodium falciparum* transcriptome prioritises genetic polymorphisms associated with artemisinin response

Andrew Walakira[1,2,14,*], Ronald Galiwango[1,2], Brenda Namugamba[1,2], Shahiid Kiyaga[1,2, 13], Kevin Cissy Nabukeera[1,2], Syrus Semawule[1,2], Edith Nabukenya[1,2], Joseph Nyanzi[1,2], Martin Okitwi[3], Stephen Orena[3], Thomas Katairo[3,11,12], Victor Asua[3], Stephen Tukwasibwe[3], Grace Kebirungi[1,2], Fredrick E. Kakembo[1,2], David Twesigomwe[9], Joaniter I. Nankabirwa[3,14], Emmanuel Arinaitwe[3], Karamoko Niaré[6,7], Jessica Briggs[4], Melisa D. Conrad[5], Isaac Ssewanyana[10], Moses Kamya[3,14], Philip J. Rosenthal[4], Samuel L. Nsobya[3], Daudi Jjingo[1,2,8]

[1] The African Center of Excellence in Bioinformatics and Data-Intensive Sciences, Hall Lane, Makerere University, Central, P.O Box 22418, Kampala, Uganda

[2] The Infectious Diseases Institute, Hall Lane, Makerere University, Central, P.O Box 22418, Kampala, Uganda

[3] Infectious Diseases Research Collaboration, Kampala, Uganda.

[4] Department of Medicine, University of California, San Francisco, CA, USA

[5] Johns Hopkins Malaria Research Institute, Department of Molecular Microbiology and Immunology, Bloomberg School of Public Health, Johns Hopkins University, Baltimore, MD, USA.

[6] Department of Pathology and Laboratory Medicine, Brown University, Providence, RI, USA.

[7] Center for Computational Molecular Biology, Brown University, Providence, RI, USA.

[8] The Department of Computer Science, College of Computing and Information Sciences, University Rd, Makerere University, Kampala, Uganda

[9] Medical Research Council/Uganda Virus Research Institute and London School of Hygiene and Tropical Medicine Uganda Research Unit, Entebbe, Uganda

[10] Department of National Health Laboratory and Diagnostic Services, Ministry of Health, Kampala, Uganda

[11] Liverpool School of Tropical Medicine (LSTM), Liverpool, UK

[12] National Malaria Reference and Research Laboratory (NMRRL), CPHL, Kampala, Uganda

[13] Department of Immunology and Molecular Biology, College of Health Sciences, Makerere University, Kampala, Uganda

[14] Department of Medicine, College of Health Sciences, Makerere University, Kampala, Uganda

*Corresponding author: adwalakira@gmail.com

Abstract

Artemisinin-based combination therapies (ACTs) have substantially reduced the global burden of malaria, but the emergence and spread of artemisinin partial resistance (ART-R) threatens these gains. Although mutations in *Plasmodium falciparum kelch13* (*pfk13*) are established mediators of ART-R, they do not fully explain variation in parasite responses, highlighting the need for complementary markers. We integrated six independent intra-erythrocytic developmental cycle (IDC) transcriptomic datasets by harmonic regression and random-effects meta-analysis, followed by network analyses, protein structural modelling, population genomics and *ex vivo* dihydroartemisinin susceptibility data, to identify candidate *P. falciparum*

polymorphisms associated with artemisinin response. The meta-analysis identified 2,842 of 5,292 genes as significantly rhythmic across the 48-hour IDC, including those encoding PfK13 and PfMDR1. Integration with whole-genome sequences of Ugandan field isolates prioritized 13 nonsynonymous variants across 10 genes, encoding PfAP2-G, PfPX1, PfACS7, PfACS1a, PfRESA3, PfDRPC and PfA8IJP together with three proteins of unknown function, all transcriptionally co-timed with *pfk13*. Polymorphisms in *pfpx1* have independently been implicated in artemisinin susceptibility, consistent with our prioritization. These candidates are potential complementary mediators of artemisinin response. Beyond them, the pipeline itself is transferable to other resistance phenotypes and periodic transcriptional programmes.

Introduction

Artemisinin-based combination therapies (ACTs) are the WHO recommended first-line treatments for uncomplicated malaria and have contributed substantially to reductions in malaria morbidity and mortality[1]. These gains are increasingly threatened by the emergence and spread of artemisinin partial resistance (ART-R) in Africa, which is associated with mutations in the *P. falciparum kelch13* (PfK13) gene[2]. Mutations in the PfK13 propeller domain have been linked to delayed parasite clearance following artemisinin treatment in clinical studies[6–8]. However, not all parasites with clinical or laboratory evidence of ART-R harbour validated PfK13 resistance-associated mutations[14–16], and these mutations do not fully explain variation in parasite responses across diverse genetic backgrounds and geographical regions[7,9–13]. Geographically distinct *P. falciparum* populations frequently evolve distinct adaptive mutations while converging on similar resistance phenotypes[13,17], suggesting that the artemisinin response can emerge from a complex molecular architecture extending beyond a single resistance locus. These considerations have driven the search for genetic polymorphisms in addition to PfK13 mutations that impact on responses to artemisinins.

Polymorphisms in proteins in addition to PfK13 have been implicated in modulating artemisinin susceptibility, including mutations in *P. falciparum* multidrug resistance protein 1 (*pfmdr1*), ferredoxin (*fd*), AP2 adaptor complex subunit μ (*pfap2-μ*), *pfcoronin*, multidrug resistance-associated protein 1 (*pfmrp1*), and phosphoinositide-binding protein 1 (*pfpx1*) [11,17–24]. Current evidence suggests that PfK13-mediated ART-R is primarily driven by impaired haemoglobin catabolism, with mutant PfK13 reducing cytostome-mediated endocytosis of host haemoglobin during the early ring stage, limiting haemoglobin delivery to the digestive vacuole and reducing free-haem generation. Because artemisinins depend on haem-catalysed activation, this reduction in haem availability lowers drug activation within the parasite and thereby diminishes drug-induced damage, allowing early ring-stage parasites to survive artemisinin exposure[25–27]. Despite these advances, candidate resistance mediators other than PfK13 have not been consistently validated across different parasite populations or incorporated into routine genomic surveillance, and there remains a need to distinguish consistent drivers of artemisinin response from associations that are specific to individual parasite populations.

Consideration of rhythmic transcription across the *P. falciparum* intra-erythrocytic developmental cycle (IDC) represents a largely unexplored tool to investigate mechanisms of ART-R. The IDC is characterized by highly coordinated waves of transcription that regulate intra-erythrocytic parasite biology, including metabolism, replication, host-cell remodelling, and drug susceptibility[28–30]. Importantly, ART-R impacts predominantly on the early ring stage, making this developmental window central to understanding parasite responses to artemisinin[31,32]. These observations suggest that resistance-associated genes should not be viewed as static molecular markers, but rather as components of temporally coordinated regulatory programmes. Therefore, incorporating rhythmic transcriptional dynamics into studies of ART-R provides an opportunity to uncover complementary resistance markers not readily captured by analyses based solely on genomic variation or static differential gene expression. This study defines a broader molecular architecture of ART-R that extends beyond PfK13 and identifies candidate markers for future functional validation.

Methods

Gene expression datasets

We analysed six publicly available *P. falciparum* transcriptomics datasets generated from synchronized blood-stage parasites sampled throughout the 48-hour IDC. All datasets were obtained from public repositories; no new sequencing was performed in this study. Four of the six, Otto et al., Broadbent et al., Chappell et al., and Subudhi et al., were produced by Illumina RNA-seq, differing chiefly in RNA enrichment, strand-specificity and amplification, while the remaining two datasets, Bozdech et al. and Painter et al., were microarray-based[28,30,33–36]. These studies were selected based on the following criteria: (i) genome-wide transcriptomic profiling with time-resolved sampling spanning the complete 48-hour IDC, at a resolution sufficient to recover observations at 8-hour intervals, and (ii) availability of gene expression matrices suitable for downstream analyses. To maximize comparability across studies, gene identifiers were harmonized using the *P. falciparum* 3D7 annotation in PlasmoDB[37,38] accessed on March 3rd 2026. Time points from each study were aligned according to the developmental timeline of the IDC and expressed as hours post-invasion (hpi), allowing direct comparison of rhythmic transcriptional patterns across datasets (Figure 1).

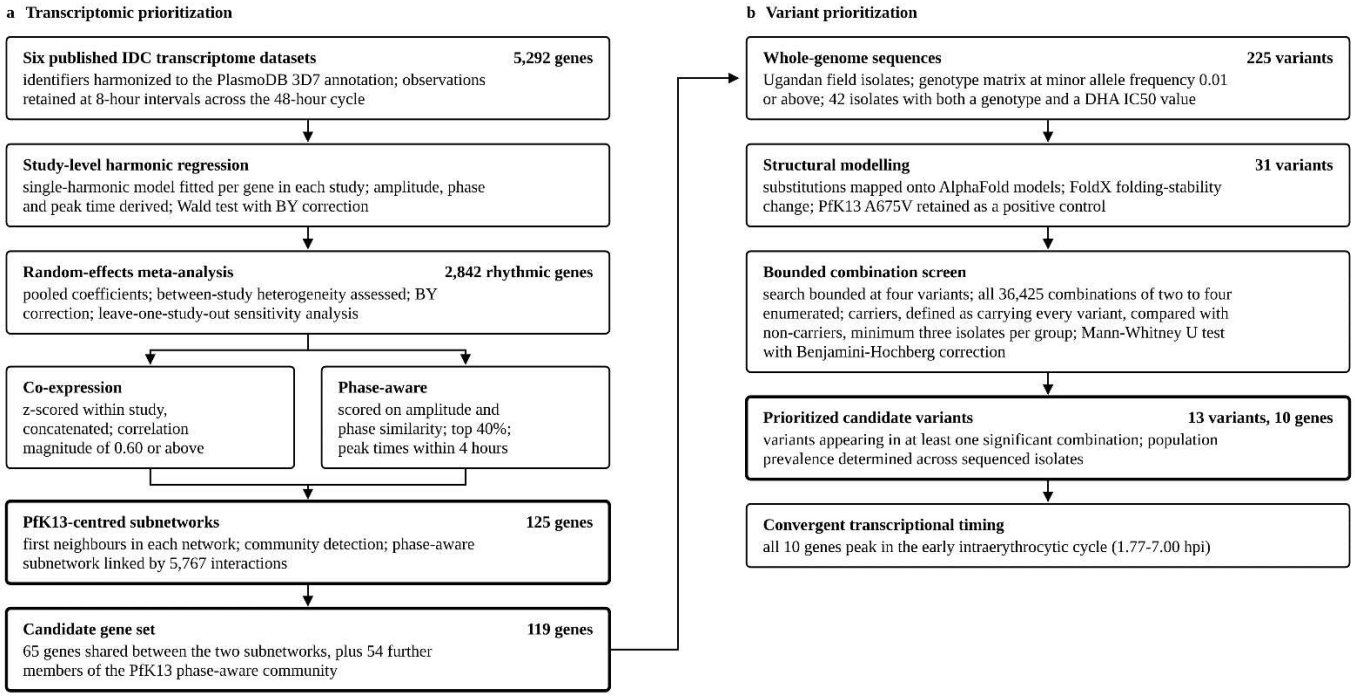


Figure 1. Integrative pipeline for prioritizing candidate variants associated with artemisinin response. (**a**) Transcriptomic prioritization. Six published intraerythrocytic developmental cycle (IDC) transcriptome datasets were harmonized to the *P. falciparum* 3D7 annotation and reduced to observations at 8-hour intervals across the 48-hour cycle. Harmonic regression was fitted per gene within each study and the resulting rhythmic parameters combined by random-effects meta-analysis. Complementary co-expression and phase-aware networks were constructed from the rhythmic genes and the first-neighbour subnetwork of PfK13 extracted from each, defining the candidate gene set. (**b**) Variant prioritization. Missense variants within those genes were identified from whole-genome sequences of Ugandan field isolates, filtered on predicted folding-stability change, and screened in combinations of up to four for association with *ex vivo* dihydroartemisinin susceptibility. Variants appearing in at least one significant combination were retained as prioritized candidates. Blue outlines mark the stages at which the candidate sets are defined; blue values give the number of genes or variants carried forward at each stage.

Study-level harmonic regression

Time-resolved transcriptomic *P. falciparum* datasets spanning the 48-hour IDC were analyzed independently using a harmonic regression framework to quantify periodic gene expression. To place all studies on a common sampling design, we retained from each dataset only those observations closest to 0, 8, 16, 24, 32, 40 and 48 hours post-invasion (hpi); observations at intermediate timepoints were not used, and no interpolation, binning or imputation was performed. All six datasets contributed observations at all seven timepoints. Where a study's sampling schedule did not include an exact grid value, the nearest available observation was used and the regression was fitted at its true recorded time rather than at the nominal grid value. Equalising the sampling design in this way prevents studies with higher native temporal resolution from dominating the pooled estimates for reasons of study design rather than biology. Because 0 and 48 hpi correspond to the same phase of the 48-hour cycle, the design comprises six distinct phases, with phase 0 sampled twice. Log_2-transformed expression at these timepoints was modelled by harmonic regression under a missing-at-random assumption. Genes with fewer than four valid observations within a given study were excluded from that study's analysis. For each gene, expression profiles were modeled using ordinary least squares regression of the form:

$$y(t) = \beta_0 + \beta_c \cos(\omega t) + \beta_s \sin(\omega t) + \epsilon$$

where: $y(t)$ is the log_2-transformed expression at time t_i, β_0 is the intercept representing baseline expression, β_c and β_s are the cosine and sine coefficients, respectively, $\omega = 2\pi/48$ represents the fundamental angular frequency of the IDC, *and* ϵ = residual error.

From the fitted model, cosine and sine coefficients (β_c and β_s) and their full variance–covariance matrix were extracted, preserving uncertainty for downstream analyses. These coefficients were transformed into biologically interpretable parameters: oscillation amplitude $A = \sqrt{\beta_c^2 + \beta_s^2}$, phase $\phi = \text{atan2}(\beta_s, \beta_c)$, and peak expression time mapped onto the 48-hour cycle $t_{peak} = (\phi \bmod 2\pi)/\omega$, Statistical significance of rhythmicity was assessed using a two-degree-of-freedom Wald test of the joint null hypothesis: H_0: $\beta_c = 0$ and $\beta_s = 0$, and resulting p-values were adjusted for multiple testing using Benjamini–Yekutieli (BY) procedure.

Meta-analysis of rhythmic transcriptional dynamics

To identify robust consensus patterns of rhythmic gene expression across independent studies, rhythmic parameters estimated from each dataset were integrated using a random-effects meta-analysis framework that combined rhythmic coefficients and derived rhythmic statistics while explicitly accounting for between-study heterogeneity. For each gene, cosine and sine coefficients from individual studies were meta-analysed separately using random-effects models, allowing for estimation of both pooled rhythmic behaviour and between-study variability. Meta-analysis pooled cosine and sine coefficients were then recombined to derive consensus rhythmic amplitude, phase and peak expression time estimates, with the modulo mapping each gene onto the interval (0, 48) hours:

$$A_{meta} = \sqrt{\hat{\beta}^2_{c,meta} + \hat{\beta}^2_{s,meta}}, \text{ and: } \phi_{meta} = \text{atan2}\left(\hat{\beta}_{s,\,meta}, \hat{\beta}_{c,\,meta}\right), t_{peak,\,meta} = (\phi_{\text{meta}} \bmod 2\pi)/\omega ,$$

These pooled rhythmic parameters allowed reconstruction of consensus IDC expression trajectories across studies. Furthermore, to evaluate the consistency of rhythmic behaviour across datasets, heterogeneity was assessed for each gene using Cochran's Q statistic, the I^2 statistic which quantifies the proportion of total variation attributable to between-study heterogeneity, and between-study variance τ^2, were calculated for each gene. Resulting p-values were adjusted for multiplicity using Benjamini–Yekutieli (BY) procedure[39].

Leave-one-study-out sensitivity analyses were additionally performed to assess robustness of rhythmic estimates and identify genes whose rhythmic behaviour was disproportionately influenced by individual studies. For each gene, changes in pooled amplitude and phase following iterative exclusion of individual

datasets were quantified. The final meta-analysis produced consensus IDC rhythmic expression profiles for each gene.

The rhythmic IDC trajectories of established antimalarial resistance genes were examined with a particular focus on *pfk13* to define its stage-specific transcriptional dynamics, rhythmic amplitude, and temporal coordination across the erythrocytic cycle. Network analysis was further used to identify genes co-expressed and phase-synchronized with *pfk13*, enabling the detection of coordinated transcriptional modules potentially linked to artemisinin response.

Construction of transcriptional co-expression and phase-aware networks

To investigate coordinated transcriptional organization, we constructed complementary co-expression and phase-aware gene–gene networks that captured similarity in expression magnitude and transcriptional timing, respectively, among rhythmic genes across the IDC. Specifically, we constructed (i) a co-expression network based on pairwise Pearson correlation coefficients calculated from gene expression profiles and (ii) a phase-aware network based on pairwise similarity in transcriptional phase among rhythmic genes. Network construction was restricted to genes showing significant rhythmic expression in the meta-analysis using a BY adjusted global rhythmicity threshold of $p < 0.05$. For each study, preprocessed expression data were filtered to retain these significant rhythmic genes. Gene-wise z-score normalization was performed independently within each study to remove differences in absolute expression while preserving temporal expression patterns. This standardization ensured that network inference reflected similarities in temporal expression patterns rather than differences in absolute expression levels. The resulting z-scored expression matrices were then aligned by gene and concatenated across studies to generate a single consensus expression matrix. Pairwise Pearson correlation coefficients were calculated from this concatenated matrix to construct the co-expression network. Edges were retained between gene pairs with strong positive or negative expression relationships, defined as Pearson's $r \geq 0.60$ or $r \leq -0.60$. Positive edges therefore represented genes with synchronized expression trajectories across the IDC, whereas negative edges represented genes with opposing expression pattern consistent with activity during different developmental stages. Together, these networks captured coordinated transcriptional relationships and biologically meaningful stage-specific regulatory patterns.

Phase-aware rhythmic coordination network

In parallel, we constructed a phase-aware rhythmic coordination network to specifically capture temporal synchronization among oscillatory genes. For each gene, meta-analysis-derived rhythmic amplitude and phase estimates were used to calculate pairwise phase-aware scores. For genes i and j, the phase-aware score was defined as the product of their rhythmic amplitudes weighted by the cosine of their phase difference: $S_{ij} = A_i A_j \cos(\Phi_i - \Phi_j)$, where A_i and A_j are the meta-analytic rhythmic amplitudes, and Φ_i and Φ_j are the corresponding rhythmic phases. High positive scores therefore indicated gene pairs that were both strongly rhythmic and temporally synchronized during the IDC. Edges in the phase-aware network were retained if their phase-aware score fell within the top 40% of all positive gene–gene scores and if the circular difference in inferred peak expression time was ≤4 hours across the 48-hour IDC. This phase constraint ensured that retained edges reflected biologically meaningful, temporal coordination rather than amplitude-driven similarity alone.

***pfk13*-centred network analysis**

To investigate transcriptional networks potentially associated with artemisinin response, a *pfk13*-centered subnetwork was extracted. The first-neighbour subnetwork was generated by retaining *pfk13* together with all directly connected genes in each network. Genes common between the conventional co-expression and phase-aware *pfk13* subnetworks were subsequently identified and prioritized for downstream analyses.

All analyses were done in Python 3.10, and networks were constructed and analysed using NetworkX[40] version 3.4.2. Filtered gene-pair edge tables were converted into undirected graphs, with correlation or phase-aware

score retained as edge attributes. Communities were detected by greedy modularity maximisation and stored as node attributes. Graphs were exported as GraphML for visualisation in Cytoscape, with accompanying SIF edge lists and Python pickle objects.

Validating the candidate genes and variants

Whole-genome sequence and drug-susceptibility data were not generated in this study but were obtained from Niaré et al.[22], where full details are reported. Briefly, isolates were collected through health facility-based surveillance across Uganda between 2016 and 2024, DNA underwent two rounds of selective whole-genome amplification and paired-end sequencing on an Illumina X Plus, variants were called with a GATK4 pipeline, and half-maximal inhibitory concentrations (IC_{50}) were determined by standardised 72-hour *ex vivo* susceptibility assays, of which only dihydroartemisinin (DHA) values were used here (accession: PRJNA1298911). Genotypes and phenotypes were matched isolate by isolate on sample identifier, giving an analysis set of 42 isolates with both a genotype and a DHA IC_{50} value. Variants within the 119 candidate genes were extracted from a genotype matrix filtered at minor allele frequency ≥ 0.01 and coded as present or absent per isolate, yielding 225 circulating missense variants. Amino acid substitutions were mapped onto AlphaFold-predicted structures[41,42] and their predicted effects on thermodynamic stability estimated as changes in Gibbs free energy ($\Delta\Delta G$) using FoldX[43] suite 5. With $\Delta\Delta G > 0$ taken as destabilizing, 31 variants were predicted to alter stability (26 destabilizing, 5 stabilizing), including the validated ART-R marker PfK13 A675V, retained as a positive control.

Association with the IC_{50} phenotype was tested for combinations of SNPs rather than for single variants alone. Exhaustive enumeration over all circulating variants was computationally infeasible, so the search was bounded at a maximum combination size of 4 variants. Preliminary analyses established four as sufficient, beyond which the proportion of combinations with enough carriers to be testable fell steeply, and the strongest associations did not improve. Therefore, larger combinations contributed no additional signal. All 36,425 combinations of two to four of the 31 structurally prioritized variants were therefore enumerated. For each combination, isolates were classified as carriers, defined as carrying every variant in that combination, or as non-carriers. Combinations with fewer than three isolates in either group were not tested. Because carrier groups are necessarily small at this sample size and IC_{50} values are right-skewed, conditions under which the distributional assumptions of parametric tests are unreliable, IC_{50} values were compared between groups using the rank-based Mann–Whitney *U* test. P-values were adjusted across the tested combinations using the Benjamini–Hochberg procedure, which controls the false discovery rate under positive regression dependence. This assumption is appropriate here because combinations are constructed from overlapping variant sets and therefore share carriers by design. Variants appearing in at least one combination significant after correction were retained as prioritized candidates. This is a screening criterion applied to combinations rather than to variants, hence retained variants are described throughout as candidates rather than as individually associated with susceptibility. The population prevalence of each retained variant was determined across all sequenced isolates. Analyses were performed in Python 3.10.

Results

We analysed six independent IDC transcriptomic datasets and identified 5,292 genes detected in at least four of the six studies, providing a common gene set for integrative rhythmic meta-analysis (Figure 1). Random-effects meta-analysis identified 2,842 genes (53.7% of the common gene set) exhibiting significant rhythmic expression across the 48-hour IDC, revealing highly coordinated temporal regulation of the *P. falciparum* blood-stage transcriptome. Between-study heterogeneity was moderate as expected across microarray and RNA-seq platforms, and was absorbed into the pooled estimates by the random-effects model. Phase estimates

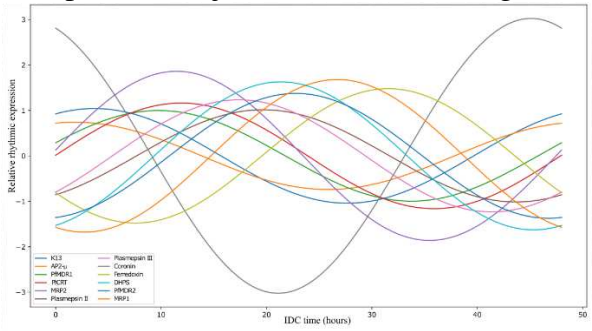
were correspondingly stable in leave-one-study-out analyses, where excluding any single dataset shifted the pooled peak expression time by less than two hours for 90.7% of genes (Supplementary Figure 1).

Established antimalarial resistance genes exhibit distinct stage-specific rhythmic expression across the IDC

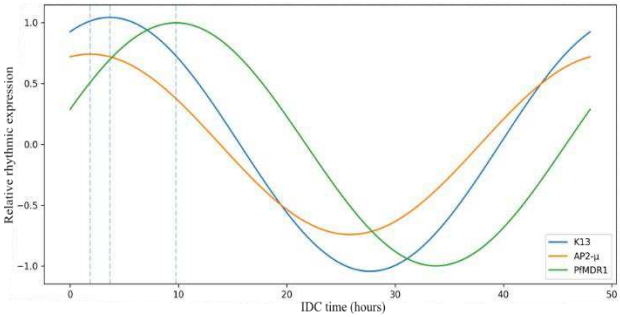
We investigated the temporal expression dynamics of established or putative antimalarial resistance-associated genes encoding PfK13, AP2-μ, PfMDR1, PfCRT, PfMRP2, PfDHPS, PfMDR2, PfMRP1, Plasmepsin II, Plasmepsin III, ferredoxin, and coronin (Figure 2, Supplementary Table 1). Each gene exhibited significant rhythmic expression across the 48-hour IDC (BY adjusted rhythmicity $p < 0.05$), indicating that known resistance determinants are embedded within the parasite's rhythmic transcriptional programme. However, their peak expression occurred at distinct developmental stages, revealing a highly organized temporal architecture in which resistance-associated pathways are sequentially activated throughout parasite development. Genes encoding the validated artemisinin resistance marker PfK13 (peak expression 3.4 hpi), and AP2-μ (0.3 hpi) reached maximal expression during the early ring stage, the developmental window during which PfK13-mediated ART-R exerts its greatest biological effect, even though artemisinins remain pharmacologically active throughout the IDC. In contrast, the genes encoding several other established or putative antimalarial resistance mediators reached maximal expression later during the IDC, including PfMDR1 (9 hpi), PfMRP2 (12 hpi), PfCRT (12 hpi), Plasmepsin III (17 hpi), Plasmepsin II (20 hpi), PfDHPS (21 hpi), PfMDR2 (23 hpi), PfMRP1 (27 hpi) and ferredoxin (32.2 hpi). This range of peak transcription across the IDC suggests that biological processes associated with antimalarial response are activated sequentially as the parasite develops.

Coronin exhibited an estimated rhythmic phase at 45.7 hpi, placing its peak in late schizogony. Since *P. falciparum* has a 48-hour life cycle, coronin's peak lies only 5.7 hours before PfK13's early ring-stage peak (3.4 hpi) across the schizont-to-ring transition. Consistent with this, coronin's transcriptional profile, like that of several other resistance-associated genes, showed elevated expression during both the early ring stage and late in the IDC. Because rhythmic phase is defined on a circular 48-hour scale, late schizogony and the early ring stage are adjacent rather than opposed, and genes peaking in this window appear elevated at both ends of a linear plot. An independent developmental time course from Mok et al.[29] shows the same early- and late-stage elevation for coronin, indicating that the pattern is a property of coronin's transcriptional timing rather than of any single culture. Residual overlap between late-schizont and early-ring parasites in synchronized cultures may nonetheless contribute.

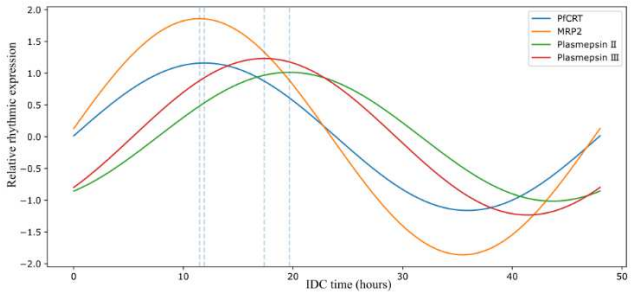
a) Expression trajectories of resistance genes



b) Early ring stage IDC expression trajectories



c) Trophozoite IDC expression trajectories



d) Schizont IDC expression trajectories

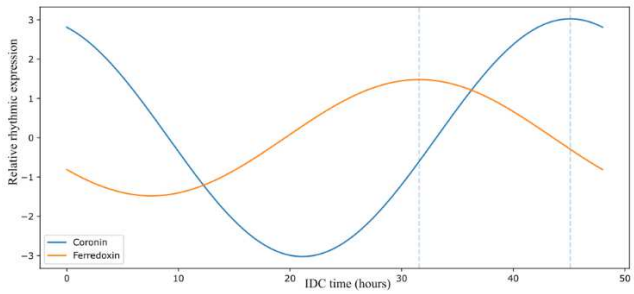


Figure 2: Stage-specific rhythmic expression profiles of established antimalarial resistance-associated genes across the 48-hour IDC. a) Rhythmic expression profiles of established resistance-associated genes. (b) Early ring-stage genes, including PfK13 and PfAP2-μ. (c) Trophozoite-stage genes, including PfMDR1, PfCRT, PfMRP2, Plasmepsins II/III, PfDHPS, and PfMDR2. (d) Late-stage genes, including ferredoxin, and coronin. These profiles demonstrate that resistance-associated genes are activated at distinct development stages, consistent with coordinated temporal transcription during the IDC.

pfk13-centred network analysis reveals coordinated transcriptional programmes associated with artemisinin response

We further investigated the transcriptional architecture associated with the validated molecular marker of ART-R, PfK13, by constructing complementary co-expression and phase-aware gene networks from the 2,842 genes exhibiting significant rhythmic expression across the 48-hour IDC. The co-expression network identified broad transcriptional communities, the two largest comprising 1,475 and 1,268 genes, respectively. PfK13 was assigned to the second-largest of these communities. Because the two largest communities together account for most rhythmic genes, it indicates only that PfK13 is not separated from the main transcriptional programme at this correlation threshold. To further refine this broad network, we constructed a complementary phase-aware network based on rhythmic phase similarity, linking genes with highly similar transcriptional timing rather than expression magnitude alone. The PfK13-centred phase-aware network comprised 125 genes connected by 5,767 synchronized interactions. Community detection within this network identified a compact PfK13-containing community of tightly phase-synchronized genes. These complementary network analyses progressively reduced the search space from thousands of rhythmically expressed genes to a focused set of transcriptionally coordinated candidates for subsequent structural, genomic, and phenotypic prioritization.

For prioritization, we first selected the 65 genes shared between the co-expression and phase-aware *pfk13* subnetworks, representing transcriptional relationships consistently supported by both analytical frameworks. We then retained all of the other 54 genes belonging to the *pfk13*-containing phase-aware community to ensure that tightly synchronized genes associated with the canonical ART-R marker were comprehensively represented in the candidate set. The two complementary selection criteria yielded a final set of 119 genes for downstream analyses. Analysis of previously generated whole-genome sequencing data from Ugandan field isolates identified, within these prioritized genes, 225 missense variants segregating at a minor allele frequency of 0.01 or above. The predicted effect of each substitution on protein stability was then assessed using FoldX. Variants were considered to alter stability where the predicted change in folding free energy exceeded 1.5 kcal/mol in either direction. Thirty-one of the 225 variants met this criterion, including the validated ART-R-associated PfK13 A675V mutation. Of these, 26 were predicted to destabilize the corresponding proteins ($\Delta\Delta G > 0$), whereas five were predicted to increase protein stability.

The 31 structurally prioritized variants were then screened against *ex vivo* dihydroartemisinin susceptibility. Of the 36,425 enumerated combinations of two to four variants, 726 had at least three isolates in each group and were tested, of which 117 showed a significant difference in IC_{50} between carriers and non-carriers after

Benjamini–Hochberg correction. The variants constituting these combinations comprised 13 missense variants across 10 protein-coding genes, which were retained as prioritized candidates (Table 1); their prevalence across sequenced isolates ranged from 14.7% to 97.1%. As expected from the phase-synchrony criterion used to define the candidate set, all ten genes peak during the early IDC (1.8–7.0 hpi), closely tracking *pfk13* at 3.4 hpi (Figure 3). Together, these analyses identify candidate variants that are transcriptionally co-timed with *pfk13*, are predicted to alter protein stability, circulate in Ugandan field isolates, and occur in combinations associated with reduced dihydroartemisinin susceptibility; none of these layers establishes a causal role, and functional validation will be required.

a) Phase profiles of identified genes

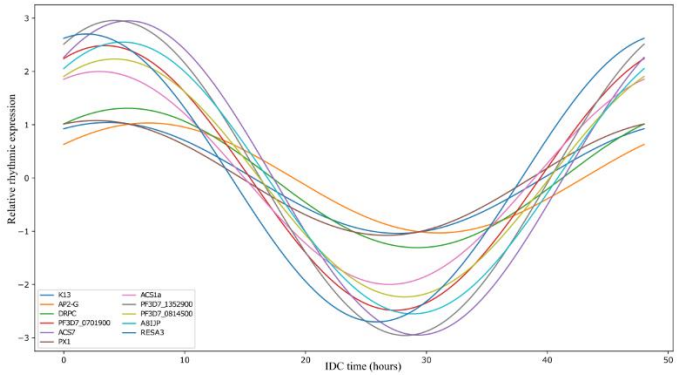


Figure 3. Expression trajectories for the 10 prioritized candidate genes together with *pfk13*. All candidate genes peak during the early IDC (1.8–7.0 hpi), within the phase window imposed by the ≤ 4-hour synchrony criterion used to define the candidate set relative to *pfk13* (3.4 hpi).

Table 1. Prioritized candidate variants associated with artemisinin response identified through the integrated pipeline. The table lists the 13 missense variants identified across 10 protein coding genes together with the gene identifier, product description, gene symbol (where available), and chromosomal location. For each candidate gene, the prioritised amino acid substitution, and the prevalence (%) of each variant among all sequenced isolates with a genotype call at that position is shown. Gene annotations were obtained from PlasmoDB accessed on March 3rd 2026.

Gene_ID	Product Description	Gene Symbol	Chromosome	Variant	Prevalence
PF3D7_0701900	Plasmodium exported protein, unknown function	-	7	S789P	19.8
				M950I	39.2
PF3D7_0720700	phosphoinositide-binding protein PX1	PX1	7	D384A	62.4
PF3D7_0814500	conserved protein, unknown function		8	N677D	91.4
PF3D7_1149200	ring-infected erythrocyte surface antigen	RESA3	11	K827N	97.1
PF3D7_1200700	acyl-CoA synthetase	ACS7	12	G387A	49.0
				A361S	52.5
PF3D7_1218500	dynamin-like protein, putative	DRPC	12	H250Y	16.8
PF3D7_1222600	AP2 domain transcription factor AP2-G	AP2-G	12	N1511K	14.7
PF3D7_1352900	Plasmodium exported protein, unknown function	-	13	F108V	78.6
PF3D7_1401100	HSPA8-interacting J protein	A8IJP	14	N480K	96.2
PF3D7_1479000	acyl-CoA synthetase	ACS1a	14	K506E	67.9
				D97G	88.5

Discussion

ART-R is one of the greatest threats to global malaria control and elimination, yet the molecular mechanisms underlying ART-R remain incompletely understood. Although *pfk13* mutations are clear mediators of ART-R, they do not fully explain the diversity of parasite responses to artemisinin-based therapy[4,17]. Thus, the response to artemisinins likely extends beyond a single resistance locus. Here, we show that established resistance-associated genes are transcribed in a coordinated rhythmic sequence across the 48-hour IDC. Across six independent datasets we defined a consensus rhythmic programme of 2,842 genes, and within it a set of 119 genes transcriptionally co-timed with *pfk13*. By integrating this rhythmic transcriptomic framework with network analysis, structural modelling, population genomics and *ex vivo* susceptibility data, we prioritized 13 candidate variants across 10 genes as potential co-mediators of ART-R. Beyond these candidates, the study provides a transferable framework for prioritizing resistance-associated genes in *P. falciparum*.

The IDC is a tightly regulated developmental programme that governs parasite replication, host-cell remodelling, metabolism, and progression through distinct developmental stages[28,30]. Although artemisinins are active against a broad range of asexual blood stages, the phenotypic impact of PfK13 mutations is most pronounced during the early ring stage, when altered haemoglobin uptake and processing reduce artemisinin activation and enhance parasite survival[25,27,32]. Because a protein is generally expressed during the developmental window in which it acts, the timing of transcription across the IDC offers a useful lens for identifying resistance-associated genes. Peak transcription marks when a gene product first becomes available and therefore sets a lower bound on when it can act hence a gene first transcribed during late schizogony cannot contribute to events earlier in that same cycle, although it may act during the rings that follow. Consistent with this, the established resistance-associated genes examined here showed distinct, stage-specific rhythmic profiles that tracked their normal biological roles rather than any shared adaptation to drug pressure. The expression of *pfk13* and *ap2-μ* genes peaked during the early ring stage (Figure 2b), while *pfcrt* and several other genes peaked later in the IDC (Figures 2c and d), matching the developmental stages in which their respective cellular functions are required. These patterns do not establish direct functional roles in ART-R, but considering transcriptional timing provides a biologically informed approach for prioritizing candidate genes and generating testable hypotheses about their potential contributions to ART-R.

Although conventional co-expression networks identify genes with similar expression profiles, they do not explicitly account for the timing of transcription. The complementary network analyses strengthened confidence in the transcriptional associations identified in this study. Community detection, which groups genes that are more densely connected to one another than to the rest of the network, placed PfK13 within broader transcriptionally coordinated gene modules. This suggests that genes associated with artemisinin response are embedded within wider developmental transcriptional programmes. Identification of the smaller phase-aware community was particularly informative because it resolved a tightly synchronized module containing several largely uncharacterized genes whose transcriptional timing closely resembled that of PfK13. These analyses provide a focused set of candidates and testable hypotheses for functional investigation to determine whether they contribute to ART-R.

Integrating complementary sources of biological evidence further facilitated prioritization of candidate markers. We combined rhythmic expression, network topology, protein structural modelling, naturally occurring genetic variation, and integrated *ex vivo* drug susceptibility data to identify the most plausible candidate genes for future functional investigation. Each analytical layer addressed a different aspect of biological plausibility. Rhythmic transcription identified genes whose expression timing resembled that of *pfk13*, network analyses prioritized genes with consistent transcriptional relationships, structural modelling identified missense variants predicted to alter protein stability, population genomic data established which variants circulate in field parasites, and *ex vivo* susceptibility data assessed whether the variants were associated with altered dihydroartemisinin susceptibility. This multi-layered strategy increased specificity by requiring support from several independent sources of evidence, although we acknowledge that this stringency may have excluded true candidates that were supported by only one or a few analytical layers. The shared early-IDC profile of the prioritized genes (Figure 3) follows from the phase-synchrony criterion used to define the candidate set. Although this is a property of the selection rather than independent evidence, it ensures that the candidates are confined to the developmental window in which PfK13-mediated ART-R is expressed. More broadly, this integrative strategy provides a systematic approach for generating a focused set of experimentally testable candidates for future mechanistic studies.

The functional diversity of the prioritized genes illustrates the breadth of biological processes represented among the candidates. The prioritized genes encode proteins involved in transcriptional regulation (AP2-G), phosphoinositide-mediated membrane signalling (PX1), membrane remodelling (DRPC, dynamin-related

protein C, annotated in PlasmoDB as a putative dynamin-like protein), host erythrocyte remodelling (RESA3), lipid activation and metabolism (ACS7 and ACS1a), and molecular chaperone function (A8IJP), together with several exported proteins whose biological functions remain poorly characterized[44] . Among the prioritized genes, *pfpx1* is notable because a study by Mukherjee et al. demonstrated that it participates in haemoglobin trafficking in *P. falciparum*, placing it within a cellular process closely linked to the established K13-mediated mechanism of ART-R[21]. More recent work provides converging genomic and functional evidence that *pfpx1* polymorphisms alter artemisinin susceptibility. Niaré et al.[22] associated a *pfpx1* haplotype (L1222P, M1701I, D1705N, plus two deletions) with decreased susceptibility in Ugandan field isolates, and Bower-Lepts et al.[45] recovered the same locus through a genetic cross of 460 recombinant progeny clones combined with *in vitro* drug selection. The PX1 substitution prioritized here (D384A) is distinct from the haplotype reported in those studies, indicating that variation at this locus associated with reduced susceptibility is not confined to a single allele. The remaining candidates should be viewed as candidates for functional testing, and it is not clear that ART-R involves all of the diverse biological processes represented in the candidate set. The identification of multiple prioritized variants within PF3D7_0701900, ACS7, and ACS1a, together with variant prevalences ranging from 14.7% for AP2-G N1511K to over 95% for variants in RESA3 and A8IJP, shows that the prioritization captured both relatively uncommon and highly prevalent polymorphisms. Variants at the upper end of this range are close to fixation in the sampled population and therefore contribute little discriminatory information since their appearance in significant combinations is likely driven by the lower-prevalence variants they accompany. Although direct mechanistic roles cannot be inferred from the present analyses, the convergence of transcriptomic, network, structural, genomic, and phenotypic evidence identifies these genes as candidates for functional validation.

The biological relevance of our candidate set of genes is further supported by independent developmental multi-omics data from Mok et al.[29] who profiled synchronized wild-type and resistance-associated K13 mutant parasites throughout the intra-erythrocytic developmental cycle. In wild-type parasites, *pfk13* exhibited maximal transcript abundance during the early ring stage (0 hpi, log2 ratio 0.89), followed by a progressive decline through trophozoite development to a minimum at 32 hpi (−0.82), with re-expression at the onset of the subsequent erythrocytic cycle (0.46 at 48 hpi), closely matching the rhythmic profile recovered by our meta-analysis. *pfcoronin* showed a similar biphasic pattern; its expression was elevated near invasion (0 hpi, log2 ratio 0.56), fell to a trough during the trophozoite stage (32 hpi, −0.58), then rose sharply during late schizogony (40 hpi, 2.41; 48 hpi, 1.73). This early-and-late elevation, close to our meta-analysis derived peak of 45.7 hpi, indicates that the late signal represents a genuine expression peak. Notably, all prioritized candidate genes displayed a broadly similar developmental transcriptional trajectory, characterized by relatively high transcript abundance during the early IDC, declining expression through trophozoite development, and renewed expression during late schizonts and the subsequent ring stage. Although the precise timing and magnitude of expression varied between genes, the overall high–low–high pattern was remarkably consistent with that observed for *pfk13*, providing independent support for the conserved temporal organization identified in the present study. Furthermore, Mok et al. identified PF3D7_1218500 *(*PfDRPC*)* as differentially expressed at both the transcript and protein levels in parasites carrying resistance-associated K13 mutations, while PF3D7_0701900 and PF3D7_1352900 were also differentially expressed at the transcript level between K13-mutant and wild-type parasites. The Mok et al. datasets were not among the six analysed here, so these agreements represent replication in an independent dataset rather than an echo of the criteria used to select the candidates.

Beyond the specific candidates reported here, the analytical framework is itself an output of this work, and three of its components transfer readily to other problems. First, the meta-analysis yields a consensus description of IDC transcriptional timing, comprising pooled amplitude, phase and peak expression time for 2,842 genes, together with heterogeneity and leave-one-study-out diagnostics (Supplementary Figure 1).

Because it draws on six datasets spanning both microarray and RNA-seq platforms, it is not tied to the idiosyncrasies of any one of them, and can be reused independently of the candidate-gene analysis reported here. Second, the phase-aware network scores gene pairs on amplitude-weighted phase similarity rather than correlation alone, and so resolves temporally coordinated modules that conventional co-expression analysis leaves buried within much larger communities. This approach is applicable to any organism with a periodic transcriptional programme. Third, the combinatorial screen tests combinations of variants directly rather than assuming additive single-variant effects, which suits populations in which variants co-segregate as haplotypes. Because these components are modular, the same framework extends to partner-drug resistance, to other *Plasmodium* species, or to any phenotype whose candidate genes are expected to act within a defined developmental window. More broadly, the framework reframes the search for resistance determinants as a question of when a gene acts rather than of sequence alone. As genomic surveillance continues to generate candidate variants faster than they can be functionally validated, prioritization schemes that draw on independent biological information, rather than statistical association alone, offer one route to closing that gap.This study identified promising candidate molecular markers associated with artemisinin response, though some limitations should be acknowledged. First, our analyses were based on previously generated transcriptomic datasets obtained under laboratory conditions and may not fully capture the transcriptional heterogeneity present in natural *P. falciparum* infections across diverse epidemiological settings. Related to this, nominal hours post-invasion are not strictly equivalent across studies, since synchronisation protocols differ e.g., six sequential sorbitol treatments in Bozdech et al., L-alanine synchronisation in Painter et al., and Percoll purification with a two-hour invasion window in Subudhi et al. So a residual inter-study phase offset of one to two hours is expected independently of any analytical choice. The random-effects framework accommodates this directly, since such offsets contribute to the between-study variance τ^2 and are therefore reflected in the heterogeneity statistics reported for each gene. They are propagated into the uncertainty of the pooled phase estimates rather than being assumed away. Second, the co-expression and phase-aware network analyses identify coordinated transcriptional patterns rather than direct regulatory or molecular interactions, and therefore cannot establish causal relationships among the prioritized genes. Third, computational predictions of protein structural stability provide indirect evidence of the potential consequences of genetic variation and cannot substitute for experimental characterization. It is not clear that polymorphisms most likely to disrupt protein stability are those likely to impact on drug susceptibility. Finally, the biological roles of these proteins in artemisinin response remain to be established through genome editing, functional genomics, biochemical characterization, and prospective phenotypic studies. Nevertheless, the convergence of multiple independent sources of evidence across complementary analytical approaches provides a compelling basis for prioritizing candidate proteins for experimental investigation.

Data availability

All datasets analysed were previously published and publicly available; no new sequencing data were generated. Six Plasmodium falciparum intra-erythrocytic developmental cycle transcriptomic datasets were obtained from Bozdech et al.[28], Otto et al.[30], Broadbent et al.[33], Chappell et al.[34], Painter et al.[35] and Subudhi et al.[36]. These can be accessed as described in the respective publications. Whole-genome sequencing data were obtained from Niaré et al.[22] (NCBI BioProject PRJNA1298911), while *ex vivo* dihydroartemisinin susceptibility data can be obtained upon reasonable request to the corresponding author.

Code availability

All code used in this study has been deposited in the GitHub repository (https://github.com/aceuganda/AIMaR). The repository includes annotated Jupyter notebooks for transcriptomic analyses, co-expression and phase-aware network construction, and pfk13-centred network analyses. Variant prioritisation and the WGS workflows are also provided as reusable Google Antigravity agent skills.

Author contributions

A.W. conceived and designed the study, led the analysis, interpreted the findings and drafted the manuscript. D.J., R.G. and S.L.N. contributed to the study design, scientific direction, interpretation of findings and critical review of the manuscript. G.K., F.K., D.T., B.N., S.K., K.C.N., S.S., E.N. and J.N. contributed to data processing, computational analyses and interpretation of results. P.J.R. made substantial contributions to the critical evaluation, revision and scientific refinement of the manuscript. M.O., S.O., T.K., V.A., S.T., K.N., J.B., M.D.C., J.I.N., E.A., I.S. and M.K. contributed to data generation, curation, scientific interpretation and critical review of the manuscript. All authors reviewed, edited and approved the final manuscript.

Competing interests

The authors declare no competing interests.

Acknowledgements

This project was supported by Google.org Social Impact (Contract ID: n302650) through the Combating Antimalarial Resistance: An AI-Driven Approach to Identify and Prioritize Key Parasite Mutations (AIMaR) grant, and the Malaria Training Programme at Makerere University through the Fogarty International Center of the National Institutes of Health under Award Number D43TW010526. Additional support was provided by the High-Performance Computing for HIV Research Excellence (HPC4HIV) grant funded by the U.S. National Institutes of Health (Award Number 1G11TW013072-01); the Data Science for Health Discovery and Innovation in Africa (DS-I Africa) – eLwazi Open Data Science Platform (Award Number 1U2CEB032224-01); the Wellcome Trust through the Centers for Antimicrobial Optimisation Network (CAMO-Net) (Award No. 226692/Z/22/Z); the Data-Driven Infrastructure for Combating Antimicrobial Resistance in Uganda (DARING) project funded by Lacuna fund and Wellcome (Grantee #103); and the She Data Science (SHEDS) program: Empowering Uganda's Women in Health Data Science: Identifying Barriers, Bridging Knowledge and Innovation for Tangible Impact through a collaborative agreement with the University of California San Francisco (UCSF) (Agreement No. UFRA-460). The content is solely the responsibility of the authors and does not necessarily represent the official views of the funders. The funders had no role in study design, data collection and analysis, the decision to publish, or the preparation of the manuscript.

References

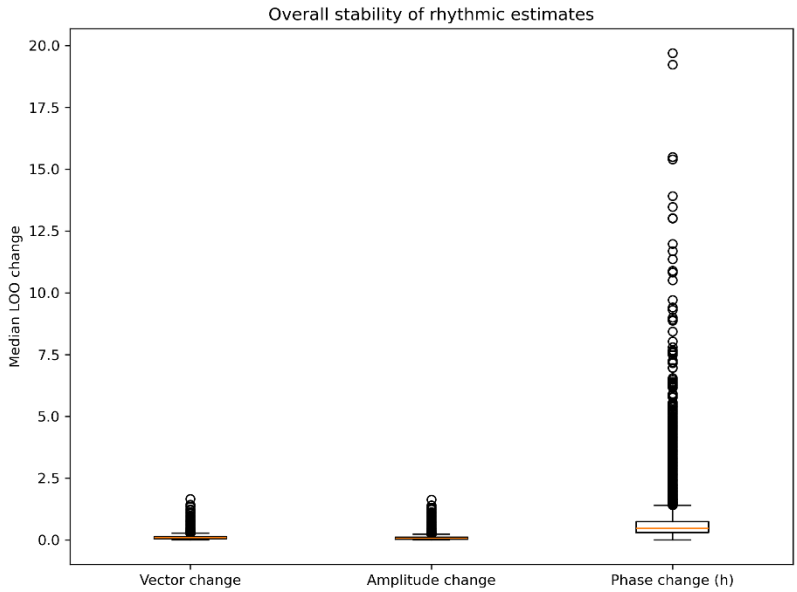
1. WHO. World malaria report 2024. https://www.who.int/teams/global-malaria-programme/reports/world-malaria-report-2024 (2024).
2. Rosenthal, P. J. *et al.* The emergence of artemisinin partial resistance in Africa: how do we respond? *The Lancet Infectious Diseases* **24**, e591–e600 (2024).
3. Balikagala, B. *et al.* Evidence of Artemisinin-Resistant Malaria in Africa. *New England Journal of Medicine* **385**, 1163–1171 (2021).
4. Conrad, M. D. *et al.* Evolution of Partial Resistance to Artemisinins in Malaria Parasites in Uganda. *New England Journal of Medicine* **389**, 722–732 (2023).
5. WWARN K13 Genotype-Phenotype Study Group. Association of mutations in the Plasmodium falciparum Kelch13 gene (Pf3D7_1343700) with parasite clearance rates after artemisinin-based treatments—a WWARN individual patient data meta-analysis. *BMC Medicine 2019 17:1* **17**, 1 (2019).
6. Ariey, F. *et al.* A molecular marker of artemisinin-resistant Plasmodium falciparum malaria. *Nature 2013 505:7481* **505**, 50–55 (2013).
7. Stokes, B. H. *et al.* Plasmodium falciparum K13 mutations in Africa and Asia impact artemisinin resistance and parasite fitness. *eLife* **10**, (2021).

8. Straimer, J. *et al.* K13-propeller mutations confer artemisinin resistance in Plasmodium falciparum clinical isolates. *Science* **347**, 428–431 (2015).
9. Maitland, K. *et al.* Intravenous Artesunate in Artemisinin-Resistant Severe Malaria in Uganda. *New England Journal of Medicine* https://doi.org/10.1056/NEJMC2517274 (2026) doi:10.1056/NEJMC2517274.
10. Milong Melong, C. S. *et al.* An overview of artemisinin-resistant malaria and associated Pfk13 gene mutations in Central Africa. *Parasitology Research 2024 123:7* **123**, 277 (2024).
11. Rosenthal, P. J., Asua, V. & Conrad, M. D. Emergence, transmission dynamics and mechanisms of artemisinin partial resistance in malaria parasites in Africa. *Nature Reviews Microbiology 2024* 1–12 (2024) doi:10.1038/s41579-024-01008-2.
12. Siddiqui, F. A. *et al.* Role of Plasmodium falciparum Kelch 13 Protein Mutations in P. falciparum Populations from Northeastern Myanmar in Mediating Artemisinin Resistance. *mBio* **11**, (2020).
13. Takala-Harrison, S. *et al.* Independent Emergence of Artemisinin Resistance Mutations Among Plasmodium falciparum in Southeast Asia. *The Journal of Infectious Diseases* **211**, 670–679 (2015).
14. Henrici, R. C., van Schalkwyk, D. A. & Sutherland, C. J. Modification of pfap2µ and pfubp1 Markedly Reduces Ring-Stage Susceptibility of Plasmodium falciparum to Artemisinin In Vitro. *Antimicrobial agents and chemotherapy* **64**, (2019).
15. Mukherjee, A. *et al.* Artemisinin resistance without pfkelch13 mutations in Plasmodium falciparum isolates from Cambodia. *Malaria journal* **16**, (2017).
16. Paloque, L. *et al.* Artemisinin pressure in field isolates can select highly resistant Plasmodium falciparum parasites with unconventional phenotype and no K13 mutation. *Antimicrobial Agents and Chemotherapy* **69**, (2025).
17. Miotto, O. *et al.* Genetic architecture of artemisinin-resistant Plasmodium falciparum. *Nature Genetics 2015 47:3* **47**, 226–234 (2015).
18. Dahlström, S. *et al.* Plasmodium falciparum Multidrug Resistance Protein 1 and Artemisinin-Based Combination Therapy in Africa. *The Journal of Infectious Diseases* **200**, 1456–1464 (2009).
19. Demas, A. R. *et al.* Mutations in plasmodium falciparum actin-binding protein coronin confer reduced artemisinin susceptibility. *Proceedings of the National Academy of Sciences of the United States of America* **115**, 12799–12804 (2018).
20. Gil, J. P. & Krishna, S. pfmdr1 (Plasmodium falciparum multidrug drug resistance gene 1): a pivotal factor in malaria resistance to artemisinin combination therapies. *Expert review of anti-infective therapy* **15**, 527–543 (2017).
21. Mukherjee, A. *et al.* A Phosphoinositide-Binding Protein Acts in the Trafficking Pathway of Hemoglobin in the Malaria Parasite Plasmodium falciparum. *mBio* **13**, (2022).
22. Niaré, K. *et al.* Emergence and spread of Plasmodium falciparum PX1 polymorphisms associated with decreased susceptibility to antimalarials in Uganda. *Nature Medicine 2026* 1–11 (2026) doi:10.1038/s41591-026-04590-5.
23. Silva, M. *et al.* Plasmodium falciparum Drug Resistance Genes pfmdr1 and pfcrt In Vivo Co-Expression During Artemether-Lumefantrine Therapy. *Frontiers in Pharmacology* **13**, 868723–868723 (2022).
24. Veiga, M. I. *et al.* Novel Polymorphisms in Plasmodium falciparum ABC Transporter Genes Are Associated with Major ACT Antimalarial Drug Resistance. *PLOS ONE* **6**, e20212–e20212 (2011).
25. Birnbaum, J. *et al.* A Kelch13-defined endocytosis pathway mediates artemisinin resistance in malaria parasites. *Science* **367**, 51–59 (2020).
26. Xie, S. C. *et al.* Haemoglobin degradation underpins the sensitivity of early ring stage Plasmodium falciparum to artemisinins. *Journal of Cell Science* **129**, 406–416 (2016).
27. Yang, T. *et al.* Decreased K13 Abundance Reduces Hemoglobin Catabolism and Proteotoxic Stress, Underpinning Artemisinin Resistance. *Cell Reports* **29**, 2917-2928.e5 (2019).

28. Bozdech, Z. *et al.* The Transcriptome of the Intraerythrocytic Developmental Cycle of Plasmodium falciparum. *PLOS Biology* **1**, e5–e5 (2003).
29. Mok, S. *et al.* Artemisinin-resistant K13 mutations rewire Plasmodium falciparum's intra-erythrocytic metabolic program to enhance survival. *Nature Communications 2021 12:1* **12**, 530 (2021).
30. Otto, T. D. *et al.* New insights into the blood-stage transcriptome of Plasmodium falciparum using RNA-Seq. *Molecular Microbiology* **76**, 12–24 (2010).
31. Klonis, N. *et al.* Altered temporal response of malaria parasites determines differential sensitivity to artemisinin. *Proceedings of the National Academy of Sciences of the United States of America* **110**, 5157–5162 (2013).
32. Witkowski, B. *et al.* Novel phenotypic assays for the detection of artemisinin-resistant Plasmodium falciparum malaria in Cambodia: In-vitro and ex-vivo drug-response studies. *The Lancet Infectious Diseases* **13**, 1043–1049 (2013).
33. Broadbent, K. M. *et al.* Strand-specific RNA sequencing in Plasmodium falciparum malaria identifies developmentally regulated long non-coding RNA and circular RNA. *BMC Genomics 2015 16:1* **16**, 454 (2015).
34. Chappell, L. *et al.* Refining the transcriptome of the human malaria parasite Plasmodium falciparum using amplification-free RNA-seq. *BMC Genomics 2020 21:1* **21**, 395 (2020).
35. Painter, H. J. *et al.* Genome-wide real-time in vivo transcriptional dynamics during Plasmodium falciparum blood-stage development. *Nature Communications* **9**, 2656 (2018).
36. Subudhi, A. K. *et al.* Malaria parasites regulate intra-erythrocytic development duration via serpentine receptor 10 to coordinate with host rhythms. *Nature Communications 2020 11:1* **11**, 2763 (2020).
37. Amos, B. *et al.* VEuPathDB: the eukaryotic pathogen, vector and host bioinformatics resource center. *Nucleic Acids Research* **50**, D898–D911 (2022).
38. Bahl, A. *et al.* PlasmoDB: the Plasmodium genome resource. A database integrating experimental and computational data. *Nucleic Acids Research* **31**, 212–215 (2003).
39. Benjamini, Y. & Yekutieli, D. The control of the false discovery rate in multiple testing under dependency. *https://doi.org/10.1214/aos/1013699998* **29**, 1165–1188 (2001).
40. Hagberg, A. A., Schult, D. A. & Swart, P. J. Exploring Network Structure, Dynamics, and Function using NetworkX. *Proceedings of the Python in Science Conference* 11–15 (2008) doi:10.25080/TCWV9851.
41. Abramson, J. *et al.* Accurate structure prediction of biomolecular interactions with AlphaFold 3. *Nature* **630**, 493–500 (2024).
42. Jumper, J. *et al.* Highly accurate protein structure prediction with AlphaFold. *Nature 2021 596:7873* **596**, 583–589 (2021).
43. Schymkowitz, J. *et al.* The FoldX web server: an online force field. *Nucleic Acids Research* **33**, W382–W388 (2005).
44. Aurrecoechea, C. *et al.* PlasmoDB: a functional genomic database for malaria parasites. *Nucleic Acids Research* **37**, D539–D543 (2009).
45. Bower-Lepts, C. *et al.* A Plasmodium falciparum PX1 haplotype is associated with reduced susceptibility to artemisinin and lumefantrine. *bioRxiv* 2026.05.05.722990-2026.05.05.722990 (2026) doi:10.64898/2026.05.05.722990.

Supplementary material

Supplementary Figure 1: Leave-one-study-out sensitivity analyses demonstrated high stability of the inferred rhythmic programmes. Exclusion of individual datasets resulted in only modest changes in rhythmic vector magnitude, oscillation amplitude, and phase estimates for the majority of genes, indicating that the observed rhythmic patterns were not driven by any single study and were broadly conserved across datasets.



Supplementary Table 1: Stage-specific peak expression timing of known antimalarial resistance-associated genes across the 48-hour intraerythrocytic developmental cycle (IDC). Most resistance-associated genes reached peak expression during the trophozoite stage, while *pfap2-μ* and *pfk13* peaked during the early ring stage, *pfmrp1* and *ferredoxin* during the trophozoite-to-schizont transition, and *coronin* during late schizogony. These results show that resistance-associated genes are activated at distinct developmental stages and form part of the parasite's temporally coordinated IDC transcriptional programme.

IDC Stage	Genes
Early ring stage (0–8 h)	*ap2-μ* (0.3 h), *k13* (3.4 h)
Early/Mid trophozoite stage (8–24 h)	*mdr1* (9.0 h), mrp2 (12.1 h), crt (12.2 h), *plasmepsin III* (17.9 h), *plasmepsin II* (20.2 h), *dhps* (21.7 h), *mdr2* (23.5 h)
Late trophozoite / schizont stage (24–36 h)	*mrp1* (27.6 h), *ferredoxin* (32.2 h)
Late schizont stage (>36 h)	*coronin* (45.7 h)